Developmental Biology 406 (2015) 247–258

Contents lists available at ScienceDirect

Developmental Biology

journal homepage: www.elsevier.com/locate/developmentalbiology

Hoxb1 regulates proliferation and differentiation of second heart field progenitors in pharyngeal mesoderm and genetically interacts with *Hoxa1* during cardiac outflow tract development

Marine Roux [a,b,1], Brigitte Laforest [a,b], Mario Capecchi [c], Nicolas Bertrand [a,b,2], Stéphane Zaffran [a,b,*]

[a] Aix Marseille Université, GMGF, 13385 Marseille, France
[b] Inserm, UMR_S910, 13385 Marseille, France
[c] Howard Hughes Medical Institute, University of Utah, Salt Lake City, UT, USA

ARTICLE INFO

Article history:
Received 9 March 2015
Received in revised form
6 August 2015
Accepted 14 August 2015
Available online 15 August 2015

Keywords:
Heart
Mouse
Hox genes
Second heart field
Congenital heart defect

ABSTRACT

Outflow tract (OFT) anomalies are among the most common congenital heart defects found at birth. The embryonic OFT grows by the progressive addition of cardiac progenitors, termed the second heart field (SHF), which originate from splanchnic pharyngeal mesoderm. Development of the SHF is controlled by multiple intercellular signals and transcription factors; however the relationship between different SHF regulators remains unclear. We have recently shown that *Hoxa1* and *Hoxb1* are expressed in a subpopulation of the SHF contributing to the OFT. Here, we report that *Hoxb1* deficiency results in a shorter OFT and ventricular septal defects (VSD). Mechanistically, we show that both FGF/ERK and BMP/SMAD signaling, which regulate proliferation and differentiation of cardiac progenitor cells and OFT morphogenesis, are enhanced in the pharyngeal region in *Hoxb1* mutants. Absence of *Hoxb1* also perturbed SHF development through premature myocardial differentiation. Hence, the positioning and remodeling of the mutant OFT is disrupted. *Hoxa1*$^{-/-}$ embryos, in contrast, have low percentage of VSD and normal SHF development. However, compound *Hoxa1*$^{-/-}$; *Hoxb1*$^{+/-}$ embryos display OFT defects associated with premature SHF differentiation, demonstrating redundant roles of these factors during OFT development. Our findings provide new insights into the gene regulatory network controlling SHF and OFT formation.

1. Introduction

Congenital heart defects (CHD) are the most common class of birth defect (Hoffman and Kaplan, 2002). Approximately one-third of CHD involve malformations of the conotruncal region (also known as the outflow tract [OFT]), which gives rise to the connection between the ventricles and the great vessels. Elongation of the OFT is a prerequisite for correct cardiac looping as well as rotation and proper alignment of the ventricles and great vessels during aortico-pulmonary septation. In the early embryo, the heart tube elongates by addition of cardiac progenitor cells lying outside the heart itself. The source of the new myocardium is a mesodermal progenitor cell population situated in splanchnic pharyngeal mesoderm termed the second heart field (SHF) (see Buckingham et al., 2005; Vincent and Buckingham, 2010; Zaffran and Kelly, 2012). Progressive addition of these cells to the cardiac poles accompanies rightward looping and heart tube elongation. During this process, SHF cells in pharyngeal mesoderm are closely apposed to cardiac neural crest cells and pharyngeal endoderm. The progressive elongation of the OFT is regulated by multiple intercellular signals and transcription factors in the pharyngeal mesoderm and adjacent cell types including pharyngeal epithelia and neural crest-derived cells (Rochais et al., 2009; Zaffran and Kelly, 2012). Direct or indirect perturbations of the SHF and/or cardiac neural crest cells are associated with OFT alignment defects such as double outlet right ventricle (DORV) and ventricular septal defects (VSD) (Cai et al., 2003; Kirby et al., 1983; Park et al., 2006; Porras and Brown, 2008; Prall et al., 2007; Ward et al., 2005). Hence, the identification and characterization of regulatory networks operating during OFT formation is essential to understand the origin(s) of CHD.

The contribution of the SHF to the heart has been followed

* Corresponding author at: Inserm, UMR_S910, Faculté de Médecine, 27 bd Jean Moulin, 13005 Marseille, France. Fax: +33 491797227.
E-mail address: stephane.zaffran@univ-amu.fr (S. Zaffran).
[1] Laboratory of Genetics and Development, Institut de Recherches Cliniques de Montréal (IRCM), Montréal, Québec, Canada.
[2] Aix Marseille Université, IBDM, CNRS UMR7288, Campus de Luminy, Marseille, 13009 France.

http://dx.doi.org/10.1016/j.ydbio.2015.08.015
0012-1606/

using the LIM transcription factor, *Islet-1* (*Isl1*), express in pharyngeal mesoderm (Cai et al., 2003; Sun et al., 2007). There is increasing evidence for the existence of sub-domains in the SHF, distinguishable by gene expression and their contribution to the heart (see Vincent and Buckingham, 2010 and Zaffran and Kelly, 2012). Gene expression and cell labeling experiments have shown that the anterior part of the SHF (aSHF, or anterior heart field), which expresses *Fibroblast growth factor* (*Fgf8*) and the *Mlc1v-nlacZ-24* (*Fgf10-nlacZ*) transgene (Kelly et al., 2001), is programmed to make OFT and right ventricular myocardium (Zaffran et al., 2004). In contrast, the posterior part of the SHF (pSHF) containing *Isl1*-positive but *Fgf10-nlacZ*-negative cells (Galli et al., 2008), contributes to both the inflow and outflow cardiac regions (Bertrand et al., 2011; Dominguez et al., 2012). We previously reported that the anterior Hox genes *Hoxa1, Hoxa3 and Hoxb1* are expressed in distinct sub-domains of the pSHF that contribute to the venous pole and the inferior wall of OFT myocardium, which subsequently gives rise to myocardium at the base of the pulmonary trunk or sub-pulmonary myocardium (Bertrand et al., 2011). Consistent with these observations, recent fate mapping and clonal analyzes experiments have confirmed that pSHF cells contribute to OFT myocardium and that sub-pulmonary and inflow tract myocardium are clonally related (Dominguez et al., 2012; Lescroart et al., 2012).

Hox genes encode a class of transcription factors that play an important role in patterning vertebrate axial development (Mallo et al., 2010; Wellik, 2009). *Hox* genes have been shown to respond to retinoic acid (RA), the active derivative of vitamin A, during early embryonic development (Duester, 2008; Niederreither and Dolle, 2008; Niederreither et al., 1999). Retinaldehyde dehydrogenase 2 (*Raldh2*) mutant embryos, which are severely impaired in their capacity to synthesize RA, develop abnormal hearts with a single ventricular chamber and highly hypoplastic sinus venosus region (Niederreither et al., 1999, 2001). Our previous work performed on *Raldh2*$^{-/-}$ null embryos has implicated the SHF as the main cardiac progenitor population affected by RA deficiency (Ryckebusch et al., 2008). In addition, manipulation of RA level and identification of a RA-response element in the *Hoxa3* promoter demonstrated that expression of anterior *Hox* genes in the pSHF and pharyngeal endoderm is directly dependent on RA signals (Bertrand et al., 2011; Diman et al., 2011). *Hoxa1* has since been shown to be required for cardiovascular development (Makki and Capecchi, 2012). Makki and Capecchi (2012) demonstrated that the expression of *Hoxa1* in precursors of cardiac neural crest cells is important for specification of these cells that contribute to great artery and OFT formation. Several *Hoxb1* mutant mouse models have been generated and analyzed (Gaufo et al., 2000; Goddard et al., 1996; Studer et al., 1996). Although *Hoxb1*-null mice die neonatally with facial nerve and muscle defects, cardiac anomalies have not been reported (Gaufo et al., 2000; Goddard et al., 1996; Studer et al., 1996). Therefore, the role of anterior *Hox* genes during heart development remains unclear.

Here we show that Hoxb1 acts in the pharyngeal region to prevent premature differentiation of the OFT myocardium from cardiac progenitors by regulating both FGF and BMP signaling. In addition, we demonstrate that loss of *Hoxa1* function does not affect SHF development. However, using compound mutant mice, we reveal that Hoxa1 and Hoxb1 act redundantly to prevent premature differentiation of cardiac progenitors contributing to the OFT. Our work identifies a novel role for anterior *Hox* genes in cardiac progenitor cells that contribute to the formation of the conotruncal (OFT) region.

2. Material and methods

2.1. Mice

All mouse experiments were carried out using protocols approved by the “comité d’éthique pour l’expérimentation animale” (Marseille ethical committee, Protocol no. 32– 08,102,012). The null alleles of *Hoxa1*^{neo} and *Hoxb1*^{GFP} (hereafter referred to as *Hoxa1*$^{-}$ and *Hoxb1*$^{-}$) have been already described (Gaufo et al., 2000; Lufkin et al., 1991). To avoid strain background effects, we crossed mice onto the C57BL/6 background. All genotypes were observed at the expected Mendelian ratios (Supplementary material, Table S1). Double heterozygous *Hoxa1*$^{+/-}$;*Hoxb1*$^{+/-}$ mice were interbred to obtain *Hoxa1*$^{-/-}$; *Hoxb1*$^{-/-}$ embryos (Table I). *Hoxb1*$^{IRES\text{-}Cre}$ knock-in mouse line and *Mlc1v-nlacZ-24, y96-Myf5-nlacZ-16 (96-16), Mef2c-AHF-Cre*, and *Rosa26*^{LacZ} transgenic lines have been previously described (Arenkiel et al., 2003; Bajolle et al., 2006; Bertrand et al., 2011; Kelly et al., 2001; Li and Lufkin, 2000; Soriano, 1999; Verzi et al., 2005). Mice were genotyped by PCR and embryos staged taking the morning of the vaginal plug as embryonic day (E) 0.5.

2.2. RNA in situ hybridization and X-gal staining

To visualize β-galactosidase activity, embryos or hearts were isolated, fixed in 4% paraformaldehyde for 20 min and incubated in X-gal solution, according to standard procedures. Embryos and hearts were photographed (Zeiss Axiozoom) as whole mount specimens and then embedded in O.C.T. and cut into 12 μm histological section before counterstaining with eosin.

Whole-mount *in situ* hybridization (WISH) was performed as previously described (Ryckebusch et al., 2010). The riboprobes used in this study were *crabp1*, *Mlc2v*, *Tbx1*, *Islet1*, *Fgf8*, *Bmp4*, and *Shh*. For WISH, hybridization signals were detected by alkaline phosphatase (AP)-conjugated anti-DIG antibodies (1/2000; Roche), followed by color development with NBT/BCIP (magenta) substrate (Promega). After staining, the samples were washed in PBS and post-fixed. Embryos were photographed using a Zeiss Axiozoom microscope coupled to an Axiocam digital camera (AxioVision 4.4, Zeiss). Three or more embryos were examined for all conditions.

2.3. Histology and Immunochemistry

Standard histological procedures were used (Ryckebusch et al., 2010). Whole mount specimens were embedded in OCT and cut at 12 μm per tissue section. α-actinin (1:500, Sigma), AP-2α (1:50, DSHB), β-galactosidase (1:500, Cappel), Caspase3 (1:300, Cell signal), GFP (1:500; Invitrogen), Islet1 (1:100, DSHB), MF20 (1:100, DSHB), phospho-extracellular signal regulated kinase (phosphor-ERK) (1:100, Cell Signaling), Phospho-histone H3 (p-HH3) (1:400,

Table I
Cardiac defects in single and compound *Hoxa1*; *Hoxb1* mutant mice.

Genotype	*n*	Alignment defects	DORV	VSD
Wild-type	38	–		–
Hoxb1$^{+/-}$	28	–		–
Hoxb1$^{-/-}$	28	7%		21%
Hoxa1$^{+/-}$	34	–		–
Hoxa1$^{-/-}$	27	–		11%
Hoxa1$^{+/-}$ *Hoxb1*$^{+/-}$	24	–		–
Hoxa1$^{+/-}$ *Hoxb1*$^{-/-}$	12	–		25%
Hoxa1$^{-/-}$ *Hoxb1*$^{+/-}$	11	–	18%	18%
Hoxa1$^{-/-}$ *Hoxb1*$^{-/-}$	3	–	67%	67%

VSD, ventricular septal defect. DORV, double outlet right ventricle.

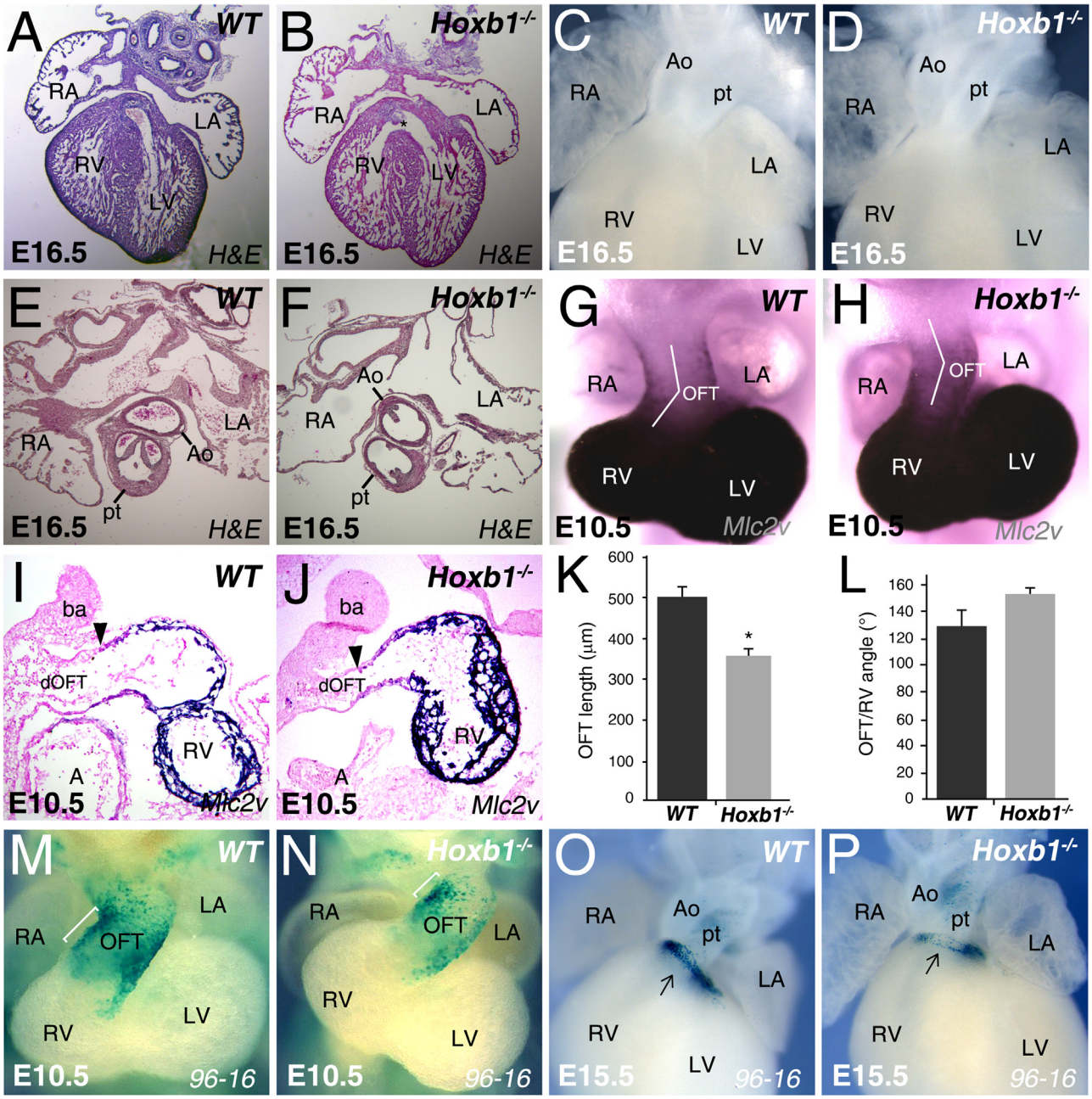

Fig. 1. Impaired development of OFT in *Hoxb1*$^{-/-}$ embryos. (A) and (B) Hematoxylin & eosin (H&E) stained sections of E16.5 wild-type (*WT*) and *Hoxb1*$^{-/-}$ hearts. Ventricular septal defects (VSD) are observed in *Hoxb1*$^{-/-}$ embryos (B; asterisk). (C) and (D) Frontal view of E16.5 hearts showing misalignment of the great vessels in *Hoxb1*$^{-/-}$ embryos. (E) and (F) Histological sections showing abnormal position of the aorta in *Hoxb1*$^{-/-}$ compared to *WT* embryos. (G) and (H) Whole-mount RNA *in situ* hybridization for *Mlc2v* (myosin light chain 2 v). Morphology of the OFT appears abnormal in *Hoxb1*$^{-/-}$ heart compared to *WT* heart. (I) and (J) Histological sections of *WT* and *Hoxb1*$^{-/-}$ embryos showing abnormal distribution of *Mlc2v* expression in the distal OFT (arrowhead). (K) and (L) Histograms showing OFT length measurements and the angle between the proximal and distal region of the OFT from *WT* ($n=9$) and *Hoxb1*$^{-/-}$ ($n=13$) hearts at E10.5 (*$p=0.0001$, Student's *t* test). (M)–(P) Ventral views of X-gal stained hearts from *WT* (M,O) and *Hoxb1*$^{-/-}$ (N,P) embryos carrying the *y96-Myf5-nlacZ-16* (*96-16*) transgene at E10.5 (M,N) and E15.5 (O,P). X-gal straining reveals reduction of 96-16 transgene expression in *Hoxb1*$^{-/-}$ (N; brackets) compared to *WT* hearts. At E15.5, β-gal positive cells are less abundant at the base of the pulmonary trunk of *Hoxb1*$^{-/-}$ (P) compared to *WT* (O) hearts (arrows). Histograms are expressed as mean ± SEM. A, atrium; Ao, aorta; LA, left atrium; LV, left ventricle; OFT, outflow tract; pt, pulmonary trunk; RA, right atrium; RV, right ventricle.

millipore), and p-Smad1/5/8 (1:100, Cell signal) immunohistochemistry were performed using 4% paraformaldehyde fixed tissue and Alexa fluorescent-conjugated secondary antibodies (Life Technologies) were used at 1:500.

2.4. Quantitative RT-PCR

The pharyngeal region, including ventral pharyngeal mesoderm and endoderm, from embryos at E9.5 were dissected in cold 1XPBS. All embryos were genotyped by PCR using yolk sac DNA. Total RNA was isolated using NucleoSpin RNA kit (Macherey-Nagel). Reverse transcriptions was performed using first strand cDNA kit (Roche). LightCycler 480 SYBR Green I Master mix (Roche) was used for quantitative real-time qRT-PCR analysis with a LightCycler 480 (Roche). Gene-specific primers used in this study were, Fgf8-For: 5′-tggaagcagagtccgagttc and Fgf8-Rev: 5′-tgtgaatacgcagtccttgc; ATP50-For: 5′-ctatgcaaccgccctgtact and ATP50-Rev: 5′-gatgataccctgggtgttgc; Bmp4-For: 5′-acaccaagcaatagccctaag

and Bmp4-Rev: 5′ggagactcattcccacctttg. Each experiment was performed in triplicate for each genotype. Samples were normalized to transcript levels of *ATP50* gene. Transcript level changes were calculated by the comparative cycle threshold (ΔΔCT) method. Normalized expression levels in the control (*Hoxb1*$^{+/+}$) were set to 1.0 for each gene.

2.5. Measurement of OFT length and angle

In situ hybridization with a *Mlc2v* riboprobe was performed on E10.5 embryos. Embryos were photographed using a Zeiss Axiozoom microscope coupled to an Axiocam digital camera (AxioVision 4.4, Zeiss). Ventral view images were taken from the same angle. The expression of *Mlc2v* was used to delimit the proximal OFT and to measure the length of the OFT. Measurement of OFT angle was made as follow: The right ventricle was encircled and the center of the circle was used as a landmark to draw a line through the middle of the proximal OFT. The OFT angle was measured at the intersection between this line and a second line passing through the middle of the distal OFT.

2.6. Statistical analysis

Statistics were carried out using Fischer's exact probability test, X^2 test for two independent samples and Student's *t* test to compare variances.

3. Results

3.1. Hoxb1 is required for cardiac OFT development

We have recently demonstrated that *Hoxb1* is expressed in a sub-population of second heart field (SHF) cardiac progenitor cells located in splanchnic pharyngeal mesoderm (Bertrand et al., 2011). At embryonic day (E) 9.5, double immunostaining confirmed that *Hoxb1* is expressed in SHF progenitors and pharyngeal endoderm where Islet1 (Isl1) is expressed (Supplemental Fig. S1). To determine if *Hoxb1* deletion was deleterious for heart development, we intercrossed *Hoxb1*$^{+/-}$ mice and collected embryos at E16.5. All wild-type (*WT*, $n=38$) and *Hoxb1*$^{+/-}$ ($n=28$) fetuses had normal cardiac morphogenesis. However, we found that six out of 28 (21%) *Hoxb1* mutants had membranous ventricular septal defects (VSD) (Fig. 1A and B and Table I) and 7% (2/28) exhibited abnormal position of the great vessels (Fig. 1C–F). These results reveal cardiac defects in absence of *Hoxb1*. Of note, although we have shown that *Hoxb1*-expressing cells also contribute to the inflow region of the heart (Bertrand et al., 2011), our morphological examination revealed no inflow tract or atrioventricular canal defects in these mutants, suggesting a functional redundancy between paralogous *Hox* expressed in pSHF cells (Bertrand et al., 2011).

The origin of the observed defects was analyzed by examining *Hoxb1*$^{-/-}$ embryos at earlier stages of cardiac development. In order to visualize the morphology of the OFT, whole-mount and section RNA *in situ* hybridizations were performed on *WT* and *Hoxb1*$^{-/-}$ embryos with a *myosin light chain 2v* (*Mlc2v*), which has differential expression levels in the proximal and distal regions of OFT myocardium (Zammit et al., 2000) (Fig. 1G–L). Expression of *Mlc2v* was abnormally detected in the distal OFT in *Hoxb1*$^{-/-}$ embryos (Fig. 1G-J; arrowhead). Consistent with these observations, OFT length was significantly reduced in *Hoxb1*$^{-/-}$ ($n=13$) compared to *WT* ($n=9$) littermates ($p=0.0001$; Fig. 1K). However, there was no difference in the angle between the proximal and distal regions of mutants OFT ($p=0.12$; Fig. 1L). Our previous study showed that SHF *Hoxb1*-expressing cells contribute to the inferior myocardial wall of the OFT (Bertrand et al., 2011). In order to visualize this sub-domain of the OFT, *Hoxb1*$^{+/-}$ mice were intercrossed with *y96-Myf5-nlacZ-16* (*96-16*) transgenic mice, in which β-galactosidase (β-gal) activity is observed in myocardial cells of the inferior OFT wall (Bajolle et al., 2006). At E10.5, X-gal staining revealed a reduction in the number of myocardial cells expressing β-gal in the OFT of *Hoxb1*$^{-/-}$ embryos (Fig. 1M and N). We found that the sub-domain of the OFT expressing the *96-16* transgene appeared to be shorter in *Hoxb1*$^{-/-}$ compared to *WT* embryos (Supplemental Fig. S2). At E15.5, *96-16* transgene expression is typically detected in the myocardium at the base of the pulmonary trunk of *WT* hearts (Fig. 1O) (Bajolle et al., 2006). Consistent with our observations at E10.5, less X-gal-positive cells were observed at the base of the pulmonary trunk of *Hoxb1*$^{-/-}$ hearts (Fig. 1P). These findings demonstrate that the *Hoxb1*$^{-/-}$ OFT is abnormal, and that the inferior OFT wall, which originates from the pSHF, is primarily affected.

3.2. Loss of Hoxb1 affects FGF signaling in the pharyngeal region

Since OFT defects in *Hoxb1* mutants are consistent with a SHF anomaly (Ward et al., 2005), we assessed the role of Hoxb1 in SHF development. We first examined the expression of a gene expressed throughout the SHF, *Islet* (*Isl1*) (Cai et al., 2003). *Isl1* transcripts were normally expressed in the SHF of *Hoxb1*$^{-/-}$ embryos (data not shown) and Isl1 protein was observed in pharyngeal mesoderm and the distal OFT of *Hoxb1*$^{-/-}$ embryos (Supplemental Fig. S3). The T-box gene *Tbx1*, genetically upstream of *Fgf10* and *Fgf8* (Abu-Issa et al., 2002; Frank et al., 2002; Vitelli et al., 2002), also displayed normal expression in the pharyngeal region of *Hoxb1*$^{-/-}$ embryos (Supplemental Fig. S3). In addition, expression of the *Mlc1v-nlacZ-24* (*Fgf10-nlacZ*) transgene, whose integration site upstream of *Fgf10* locus results in transcriptional activation of the transgene in pharyngeal mesoderm (Kelly et al., 2001), exhibited no obvious alteration in *Hoxb1*$^{-/-}$ embryos (Supplemental Fig. S3). Consistent with this, activity of *Mef2c-AHF-Cre* transgene, expressed in the aSHF (Verzi et al., 2005), was indistinguishable in *Hoxb1*$^{-/-}$ compared to control littermates (Supplemental Fig. S3).

We subsequently investigated FGF signaling, which is known to regulate the contribution of SHF-derived cells to the developing OFT. *Fgf8* transcripts, which are normally expressed in the lateral pharyngeal endoderm, surface ectoderm and, at low level, in lateral pharyngeal mesoderm (Fig. 2A and C) (Ilagan et al., 2006; Kelly et al., 2001), accumulated abnormally in ventral pharyngeal mesoderm in the dorsal pericardial wall of *Hoxb1*$^{-/-}$ embryos (Fig. 2B and D). Quantitative real-time (qRT)-PCR using tissue isolated from anterior pharyngeal regions at E9.5 confirmed an up-regulation of *Fgf8* transcript levels in *Hoxb1*$^{-/-}$ compared to control embryos (Fig. 2E). In order to analyze the extent of FGF signaling in normal expression in the pharyngeal region embryos, we performed immunostaining for phosphorylated ERK1/2 (p-ERK), kinase effectors of the MAP signaling pathway whose phosphorylation correlates with the activity of FGF8 in early heart development (Corson et al., 2003; Ilagan et al., 2006). At E9.5, when p-ERK staining is normally absent in pharyngeal mesoderm (Fig. 2F) (Ilagan et al., 2006), an increased number of p-ERK-positive cells was observed in the dorsal pericardial wall of *Hoxb1*$^{-/-}$ embryos (Fig. 2G–I), consistent with elevated FGF signaling. To investigate whether activation of FGF signaling results in elevated cell division we performed immunostaining for phosphorylated histone H3 (p-HH3), a mitotic maker. We found that the mitotic index of SHF cardiac progenitor cells (Isl1 and p-HH3 double positive cells) in *Hoxb1* mutant embryos ($n=4$) was significantly increased (40%; $p<0.05$) compared to *WT* embryos ($n=4$) (Fig. 2J–M). The number of p-HH3-positive cells was also increased in the

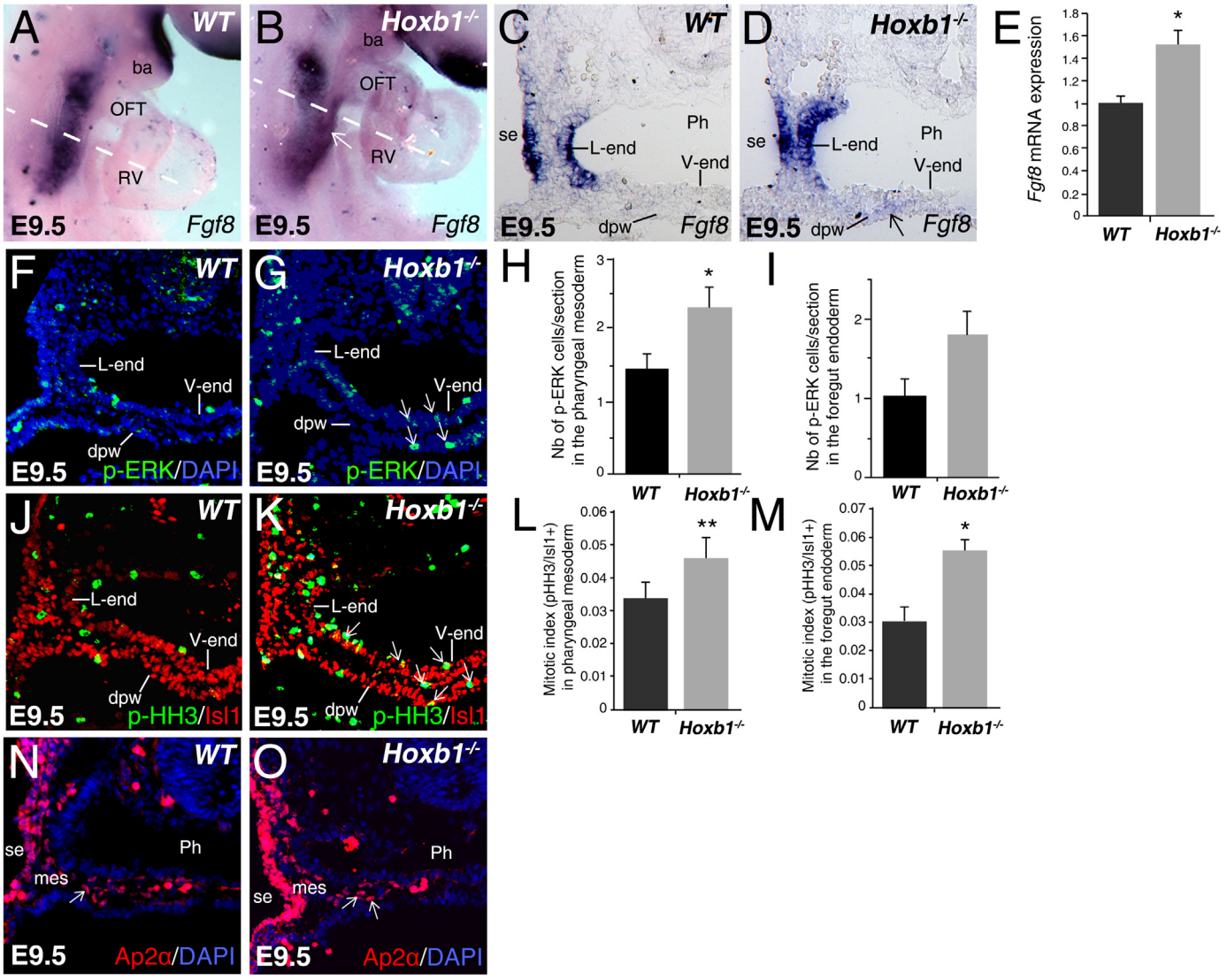

Fig. 2. Absence of *Hoxb1* disrupts FGF/ERK signaling and increases proliferation in foregut endoderm and SHF mesoderm. (A)–(D) Whole-mount *in situ* hybridization (A) and (B) and corresponding transverse sections (C) and (D) showing ectopic *Fgf8* expression in the pharyngeal mesoderm (or dorsal pericardial wall) of *Hoxb1*$^{-/-}$ embryos (arrow) at E9.5. (E) Real-time qPCR was performed from isolated pharyngeal region of E9.5 *Hoxb1*$^{-/-}$ and wild-type (*WT*) embryos. This analysis demonstrates significantly increased levels of Fgf8 gene in *Hoxb1*$^{-/-}$ vs. *WT* embryos. (F) and (G) Immunochemistry with anti-phospho-ERK antibody (p-ERK, green) in transverse sections through the caudal pharyngeal region of E9.5 *WT* and *Hoxb1*$^{-/-}$ embryos. Note the increased number of p-ERK positive cells in the ventral pharyngeal mesoderm and endoderm of *Hoxb1*$^{-/-}$ (arrows). (H) and (I) Histograms comparing the number of p-ERK-positive cells per section ($n=8$) in the pharyngeal mesoderm (H) and foregut endoderm (I) of *WT* ($n=3$) and *Hoxb1*$^{-/-}$ ($n=3$) embryos. An increase in p-ERK-positive cells is observed in *Hoxb1*$^{-/-}$ pharyngeal mesoderm and endoderm ($^{*}p<0.05$, Student's *t* test). (J) and (K) Immunochemistry with anti-phospho-Histone H3 (p-HH3, green) and anti-Isl1 (Isl1, red) antibodies in transverse sections of E9.5 *WT* and *Hoxb1*$^{-/-}$embryos; arrows points to Isl1/pHH3 double-positive cells in both pharyngeal mesoderm and endoderm. (L) and (M) Histograms comparing the mitotic index in the pharyngeal mesoderm (L) and foregut endoderm (M) of *WT* and mutants at 9.5. An increase of the mitotic index is observed in both pharyngeal mesoderm and endoderm ($^{**}p<0.05$; $^{*}p<0.02$, Student's *t* test). (N) and (O) Immunochemistry with anti-AP-2α antibody (red) in transverse sections of E9.5 embryos showing presence of neural crest-derived mesenchyme in *Hoxb1*$^{-/-}$ embryos. Nuclei are labeled with DAPI (blue). Histograms are expressed as mean ± SEM. ba, branchial arch; dpw, dorsal pericardial wall;; L-end, lateral pharyngeal endoderm; mes, pharyngeal mesenchyme; OFT, outflow tract; Ph, pharynx; RV, right ventricle; se, surface ectoderm; V-end, ventral pharyngeal endoderm.

ventral pharyngeal (foregut) endoderm of *Hoxb1*$^{-/-}$ embryos (Fig. 2L and M; $p<0.04$), suggesting persistence of active FGF signal in this layer after E9 in the absence of *Hoxb1*. We also examined apoptosis of the cardiac progenitor cells by performing immunostaining for cleaved Caspase 3. We found equivalent low numbers of Caspase 3-positive cells in the pharyngeal region of *Hoxb1*$^{-/-}$ and *WT* embryos, suggesting that apoptosis levels are unaltered (data not shown).

It has been shown that FGF8 signaling is elevated after neural crest ablation in chick embryos (Waldo et al., 2005a, Huston et al., 2006). To evaluate potential changes in the number of neural crest-derived mesenchymal cells in the pharyngeal region of *Hoxb1* mutant embryos, we examined the expression of AP-2α, a marker of migrating neural crest cells. Immunostaining for AP-2α showed that neural crest-derived cells appeared normal in number and were located in direct apposition to SHF cells and they (Fig. 2N and O).

3.3. Deletion of Hoxb1 results in premature differentiation of cardiac progenitors

It has previously been demonstrated that BMP-SMAD1 signaling induces cardiac differentiation during OFT elongation and antagonizes FGF signals (Dyer and Kirby, 2009; Hutson et al., 2010; Prall et al., 2007; Tirosh-Finkel et al., 2010; Wang et al., 2010). Therefore, we examined the expression of *Bmp4*, known to be crucial during OFT development (Liu et al., 2004). Although, *in situ* hybridization suggested a slight increase of *Bmp4* expression in the

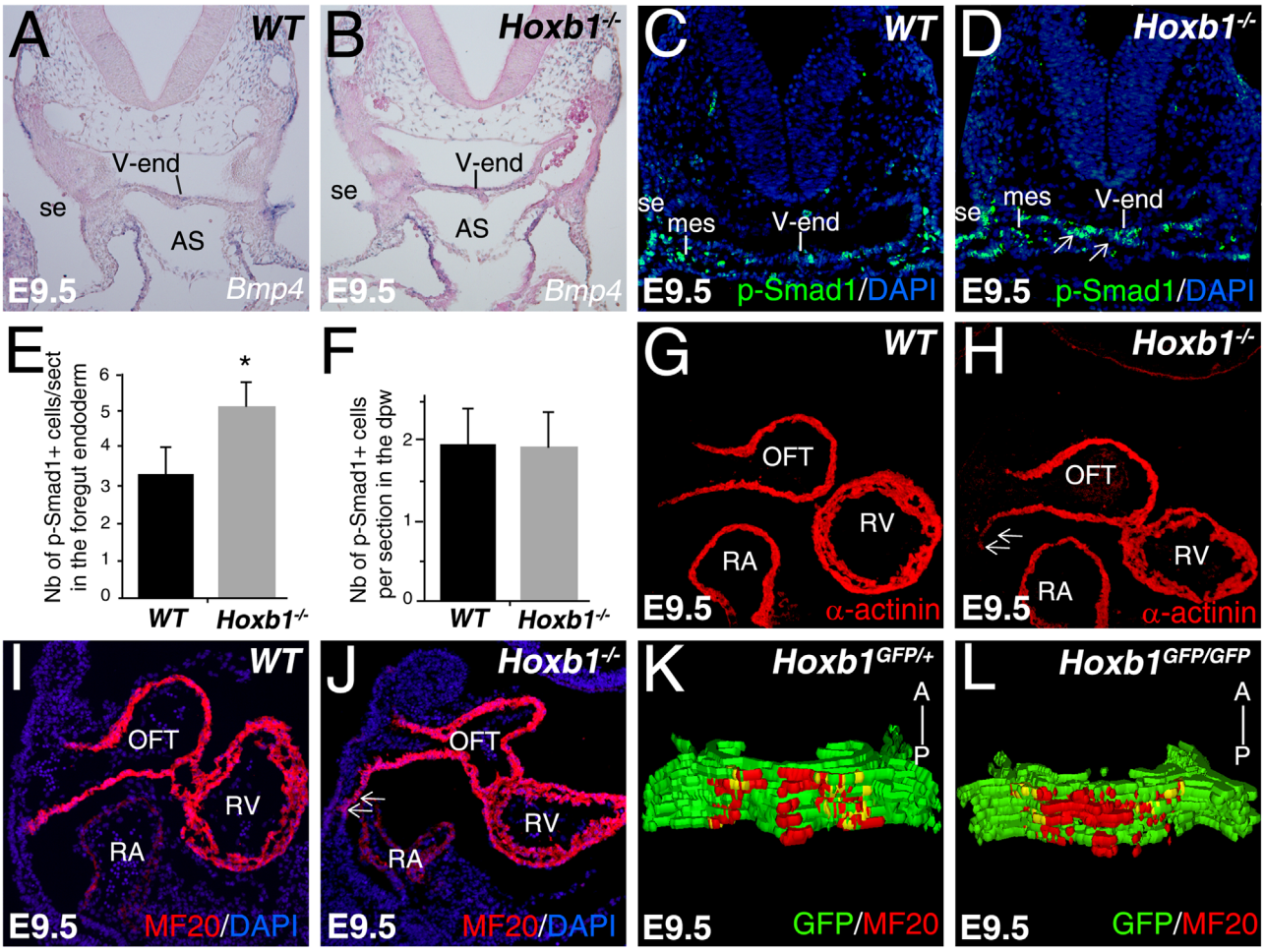

Fig. 3. Loss of Hoxb1 induces premature differentiation of SHF progenitor cells. (A) and (B) RNA *in situ* hybridization analysis of *Bmp4* in *Hoxb1*$^{-/-}$ and wild-type (*WT*) embryos at E9.5. (C) and (D) Immunochemistry with anti-phospho-Smad1/5/8 antibody (p-Smad1, green) in transverse sections of E9.5 embryos reveals increased p-Smad1 expression in the ventral endoderm of mutant embryos (arrows). (E) and (F) Histograms comparing the number of p-Smad1-positive cells per section ($n=8$) in the pharyngeal endoderm (E) and the dorsal pericardial wall (dpw, F) of E9.5 *WT* ($n=3$) and *Hoxb1*$^{-/-}$ ($n=3$) embryos. Note the increased number of p-Smad1-positive cells in the foregut endoderm (*$p<0.05$, Student's *t* test). (G)–(J) Sagittal sections of *WT* and *Hoxb1*$^{-/-}$ embryos at E9.5 labeled with anti-α-actinin (G) and (H) and anti-MF20 (I) and (J). Note the expression of differentiated cardiomyocytes in the SHF caudally to the outflow tract in *Hoxb1*$^{-/-}$ embryos (arrows). (K) and (L) Three-dimensional reconstructions of the dorsal pericardial wall show an increased number of MF20-positive cells in *Hoxb1*$^{-/-}$ embryos. Nuclei are labeled with DAPI (blue). Histograms are expressed as mean ± SEM. A, anterior; AS, aortic sac; L-end, lateral pharyngeal endoderm; mes, pharyngeal mesenchyme; OFT, outflow tract; P, posterior; ph, pharynx; RA, right atrium; RV, right ventricle; se, surface ectoderm; V-end, ventral pharyngeal endoderm.

ventral endoderm of *Hoxb1*$^{-/-}$ embryos (Fig. 3A and B), quantitative RT-PCR analysis did not confirm such difference (data not shown). However, elevated phospho-Smad1/5/8 (p-Smad1) labeling was observed in the ventral endoderm of *Hoxb1* null mutants (Fig. 3C–F). Another marker of ventral pharyngeal endoderm, *Shh*, required for SHF development, was present at normal levels in the ventral foregut of *Hoxb1* mutant embryos (Supplemental Fig. S4).

At E9.5, cells in the SHF do not express cardiomyocyte markers. Surprisingly, cells in the SHF of the *Hoxb1* mutant expressed α-actinin and MF20, two differentiation markers, before reaching the OFT (Fig. 3G–J; arrows). We found a 2.5 fold increase in the number of α-actinin-positive cells in the anterior region of the SHF (Supplemental Fig. S5), suggesting premature differentiation of cardiac progenitor cells that normally contribute to the inferior OFT wall. In order to better visualize this premature differentiation we generated three-dimensional (3D) reconstructions of MF20-positive and GFP-positive cells using a *Hoxb1*^{GFP} allele at E9.5 (Fig. 3K and L; Supplemental Fig. S5). 3D reconstruction was limited to the pharyngeal region located caudally to the OFT (Supplemental Fig. S5). 3D reconstruction displayed a clear increase of MF20-expressing cells in the dorsal pericardial wall caudal to the OFT of the mutants. Overall, these results indicate that *Hoxb1* plays an important role in the balance between proliferation and differentiation in the pharyngeal region during OFT development.

3.4. *Hoxa1 does not affect SHF and OFT morphogenesis*

Hoxa1 expression overlaps partially with that of *Hoxb1* in the pSHF (Bertrand et al., 2011). We observed that a fraction of *Hoxa1*$^{-/-}$ embryos had VSD at E17.5 (Table I), consistent with the results of Makki and Capecchi, 2012. We investigated whether loss of *Hoxa1* affected OFT morphology at E9.5 and E10.5. We found that *Hoxa1*$^{-/-}$ embryos exhibited no obvious abnormalities in OFT morphology at E9.5, as revealed by similar OFT length between *WT* ($n=4$) and *Hoxa1*$^{-/-}$ ($n=4$) embryos (Supplemental Fig. S6). Since *Hoxa1* is expressed in precursors of cardiac neural crest cells and is required for their specification (Makki and Capecchi, 2012), we examined the expression of *Crabp1*, a marker of migrating neural crest cells, at E9.5 (Fig. 4A and B). Consistently with previous reports, *Hoxa1*$^{-/-}$ embryos exhibited a strongly reduced, but still detectable, expression of *Crabp1* in the 2nd pharyngeal arch (Fig. 4A and B). In addition, streams of migrating neural crest cells appeared disorganized in *Hoxa1*$^{-/-}$ mutants (Fig. 4A and B; arrowheads). To assess whether neural crest-derived cells were

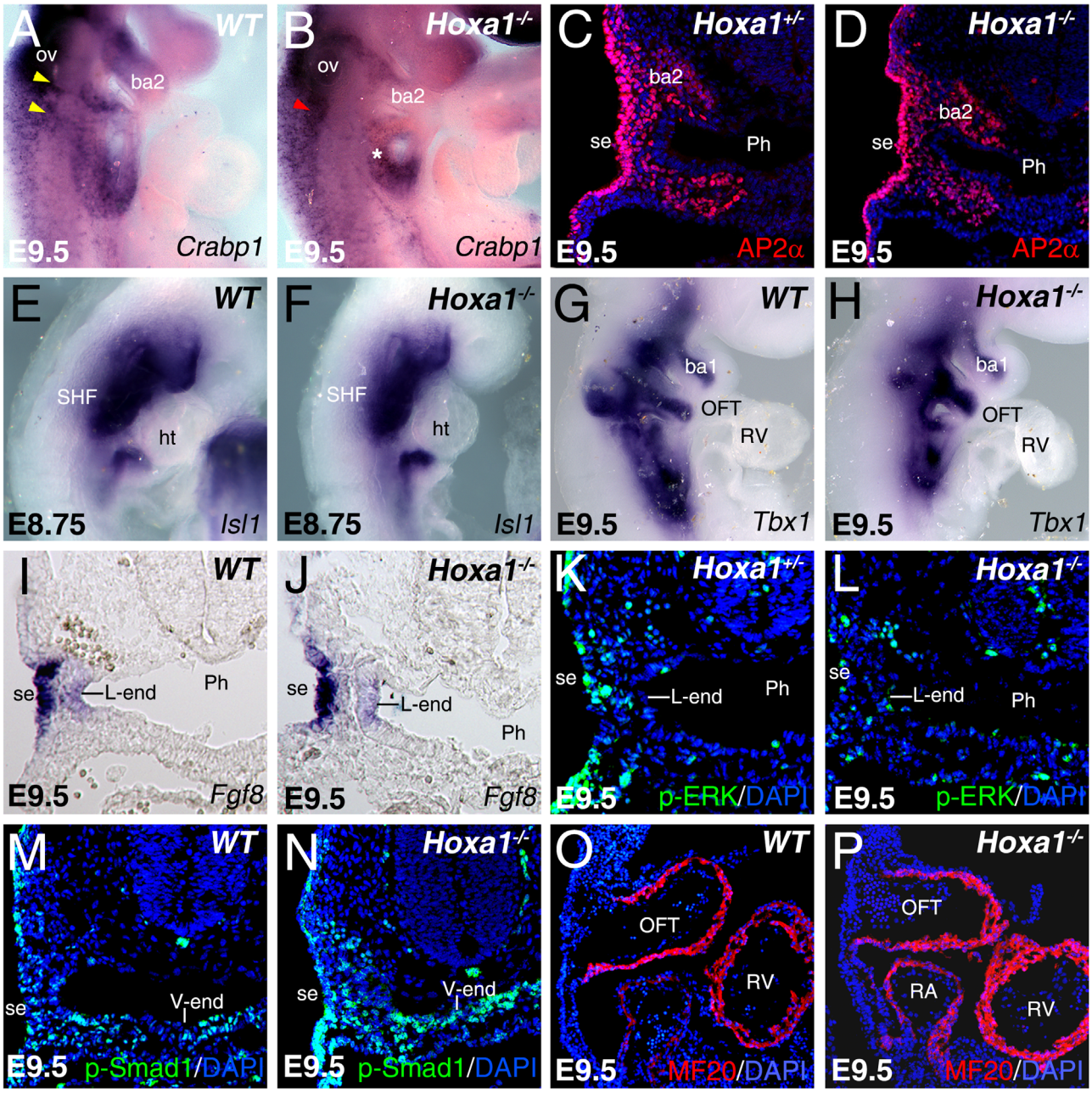

Fig. 4. Neural crest and SHF development in*Hoxa1*embryos. (A) and (B) Whole-mount *in situ* hybridization for *Crabp1* showing migrating cardiac neural crest cells in wild-type (*WT*) and *Hoxa1*$^{-/-}$ embryos at E9.5. Yellow and red arrowheads indicate normal and abnormal post-otic streams of migrating neural crest cells, respectively. (C) and (D) Immunochemistry with anti-AP-2α antibody (red) in transverse sections of E9.5 embryos reveals the presence of neural crest cells-derived mesenchyme in *Hoxa1*$^{-/-}$ embryos. (E)–(H) Whole-mount *in situ* hybridization for *Isl1* (E) and (F) and *Tbx1* (G) and (H) mRNA on E8.75 and E9.5 embryos. Expression of SHF markers appears unaffected in absence of *Hoxa1*. (I) and (J) Transverse sections of *WT* and *Hoxa1*$^{-/-}$ embryos showing normal expression of *Fgf8*. (K) and (L) Immunochemistry with anti-phospho-ERK antibody (p-ERK, green) in transverse sections of E9.5 embryos shows no elevated activity of Fgf signaling in *Hoxa1*$^{-/-}$ compared to *WT* embryos. (M) and (N) Immunochemistry with anti-p-Smad1/5/8 antibody (p-Smad1, green) do not reveal an elevated activation of BMP signaling in the ventral pharyngeal endoderm of *Hoxa1*$^{-/-}$ embryos. (O and P) Immunochemistry with anti-MF20 antibody (red) reveals no differentiated cells in the SHF of *Hoxa1*$^{-/-}$ embryos. Nuclei are labeled by DAPI (blue). ba, branchial arch; dpw, dorsal pericardial wall; L-end; lateral endoderm; mes, pharyngeal mesenchyme; OFT, outflow tract; Ph, pharynx; RV, right ventricle; V-end, ventral pharyngeal endoderm; se, surface ectoderm.

located in the pharyngeal region close to the SHF, we labeled neural crest cells with an AP-2α antibody. We found, a large number of AP-2α–positive cells within the pharyngeal region of *Hoxa1*$^{-/-}$ embryos (Fig. 4C and D; see also asterisk in Fig. 4B). These observations suggest normal neural crest-derived cell contributions to OFT septation in *Hoxa1*$^{-/-}$ embryos. Next we examined the expression of SHF markers *Isl1* and *Tbx1*. We found no major difference in *Isl1* and *Tbx1* expression in *Hoxa1*$^{-/-}$ embryos (Fig. 4E–H). Of note, *Hoxa1*$^{-/-}$ embryos exhibited hypoplasia of the posterior pharyngeal arches. In contrast to *Hoxb1*$^{-/-}$ embryos, *Fgf8* expression was normal in the pharyngeal region of *Hoxa1*$^{-/-}$ embryos (Fig. 4I and J; Supplemental Fig. S7) and this was confirmed by p-ERK labeling analysis (Fig. 4K and L; see Fig. 6E and F for quantification). Immunohistochemistry performed with p-Smad1 did not reveal dramatic difference between *WT* and *Hoxa1*$^{-/-}$ embryos (Fig. 4M and N; see Fig. 6G and H for the quantification). Consistently, MF20 immunostaining revealed no premature differentiation in the SHF of *Hoxa1*$^{-/-}$ embryos (Fig. 4O and P). Together these findings suggest that SHF development is normal in *Hoxa1*$^{-/-}$ embryos.

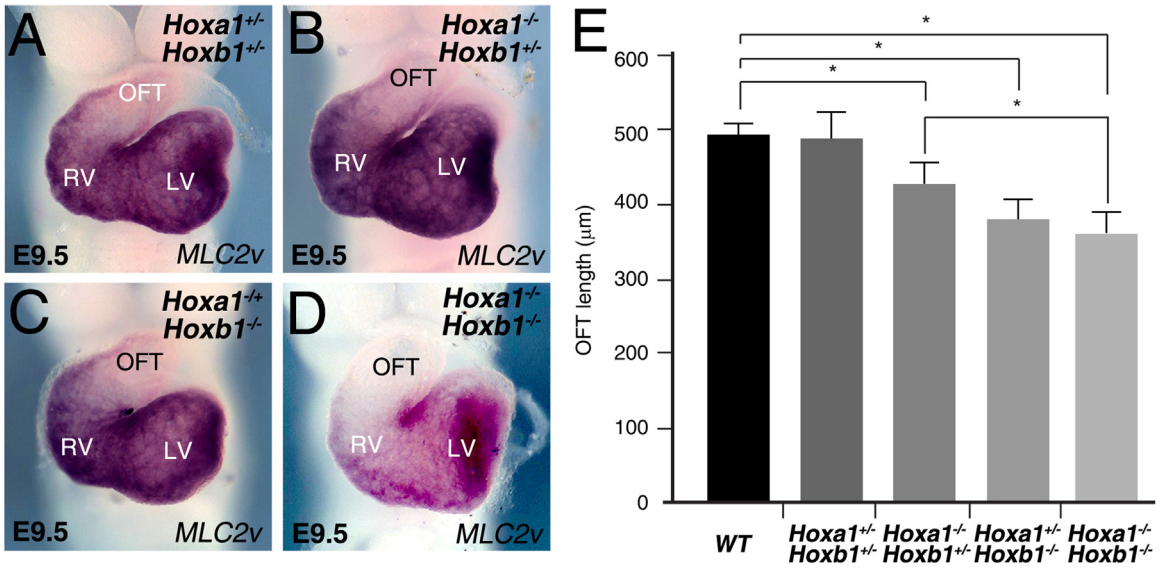

Fig. 5. OFT defects in compound *Hoxa1*;*Hoxb1* mutants. (A) and (D) Whole-mount *in situ* hybridization for *Mlc2v* at E9.5 in compound *Hoxa1; Hoxb1* embryos. Heart morphology in *Hoxa1*$^{-/-}$;*Hoxb1*$^{-/-}$ embryos appears abnormal compared to other compound embryos. (E) Histogram showing quantitative measurements of OFT length from *WT* and compound *Hoxa1; Hoxb1* hearts at E10.5 using ImageJ. Quantification confirms abnormal OFT development in the absence of two copies of *Hoxa1* and one copy of *Hoxb1*. Histograms are expressed as mean ± SEM. All measures were calculated from $n=3$ embryos for each genotype. *$p<0.05$ evaluated by Student's *t* test. OFT, outflow tract; LV, left ventricle; RV, right ventricle.

3.5. Compound Hoxa1; Hoxb1 mutants have OFT defects

Since *Hoxa1* and *Hoxb1* have overlapping expression patterns and functional redundancy during early development (Gavalas et al., 1998; Rossel and Capecchi, 1999), we asked whether removing both *Hoxa1* and *Hoxb1* would exacerbate heart defects observed in the single mutants. Double *Hoxa1*$^{+/-}$; *Hoxb1*$^{+/-}$ heterozygous mice were crossed together and a total of 115 fetuses were examined at E17.5. All genotypes, except *Hoxa1*$^{-/-}$; *Hoxb1*$^{-/-}$ (3/115 observed vs 7/115 expected), were recovered according to Mendelian ratios suggesting an early lethality of a number of double homozygous embryos ($p<0.05$ using X^2 or Fisher's test, Supplemental material Table S1 and S2). While no heart anomalies were observed in single or compound *Hoxa1*$^{+/-}$ and *Hoxb1*$^{+/-}$ heterozygous fetuses, we found that the penetrance of VSDs was significantly increased when one *Hoxa1* allele was removed in *Hoxb1*$^{-/-}$ embryos (Table I; $p<0.05$). Furthermore, deletion of one or two functional copies of *Hoxb1*^{GFP} from *Hoxa1* mutant homozygotes greatly exacerbated the heart phenotype and generated DORV, a cardiac defect not seen in single mutant embryo (Table I).

We further examined OFT morphology at E9.5 by whole-mount ISH and measured OFT length in compound *Hoxa1; Hoxb1* mutants (Fig. 5). The OFT length in *Hoxa1*$^{-/-}$ (Supplemental Fig. S6), and *Hoxa1*$^{+/-}$;*Hoxb1*$^{+/-}$ embryos (Fig. 5) was indistinguishable from that of *WT* littermates. Interestingly, significant shortening of the OFT was observed in *Hoxa1*$^{-/-}$;*Hoxb1*$^{+/-}$ embryos (Fig. 5), suggesting that deployment of SHF cells is affected in these mutants. Of note, removal of one supplementary copy of *Hoxb1* in this context did not exacerbate the phenotype compared to *Hoxb1*$^{-/-}$ mutant embryos alone (Fig. 1K compared to Fig. 5). Taken together, our results demonstrate that *Hoxa1* and *Hoxb1* interact genetically during formation of the cardiac OFT.

3.6. Disruption of pharyngeal signaling in compound Hoxa1$^{-/-}$; Hoxb1$^{+/-}$ mutants

Since we identified OFT defects in compound mutants we further examined the expression of FGF/ERK and BMP/SMAD1 signaling in the pharyngeal region of these embryos. Immunohistochemistry and quantification were performed with p-ERK and p-Smad1 on transverse sections of *Hoxa1*$^{+/-}$; *Hoxb1*$^{+/-}$ and *Hoxa1*$^{-/-}$;*Hoxb1*$^{+/-}$ embryos at E9.5 (Fig. 6A–H). In contrast to *Hoxa1*$^{-/-}$ embryos (Fig. 4L), we found an excessive number of p-ERK-positive cells in the pharyngeal region of *Hoxa1*$^{-/-}$; *Hoxb1*$^{+/-}$ embryos (Fig. 6B,E and F). Importantly, we did not detect elevated p-ERK-positive cell numbers in *Hoxa1*$^{+/-}$; *Hoxb1*$^{+/-}$ embryos (Fig. 6A,E and F). Quantification of cells positive for p-Smad1 staining revealed no significant difference between controls and compound mutant embryos (Fig. 6D,G and H). Interestingly, MF20-positive cells were detected in the aSHF of *Hoxa1*$^{-/-}$;*Hoxb1*$^{+/-}$ embryos (Fig. 6J). No ectopic MF20-expressing cells were found in the dorsal pericardial wall caudal of double heterozygous embryos (Fig. 6I). Together these data reveal a genetic interaction between *Hoxa1* and *Hoxb1* in the regulation of signaling pathways in the SHF during OFT development.

4. Discussion

In this study, we have shown that absence of *Hoxb1* causes abnormal morphology of the cardiac OFT, and subsequent ventricular septal defect (VSD) as well as partially penetrant misalignment of the great vessels.

4.1. Hoxb1 regulates intercellular signaling pathways in the pharyngeal region

OFT elongation involves progressive addition of progenitor cells from the SHF, which requires precise temporal regulation of SHF cell proliferation and differentiation. Modulation of FGF signaling in pharyngeal mesoderm of *Hoxb1*$^{-/-}$ embryos was revealed by elevated p-ERK levels in ventral splanchnic mesoderm located caudally to the OFT. This increased activation of FGF signaling is likely to promote the increased cell proliferation observed in the pharyngeal region of *Hoxb1*$^{-/-}$ embryos. This is consistent with the role of FGF8 as the major FGF ligand controlling proliferation in pharyngeal mesoderm and endoderm (Ilagan et al., 2006; Park et al., 2006; Watanabe et al., 2010).

A precise level of FGF8 signaling has been associated with

regulating proliferation rate in myocardial progenitor cells in the avian SHF. Interestingly, ablation of cardiac neural crest in chicken embryos causes a functional increase in FGF signaling (Farrell et al., 2001; Hutson et al., 2006) and increased *Fgf8* transcript levels were observed in the caudal pharynx of neural crest-ablated embryos (Hutson et al., 2006). In addition, ablation of cardiac neural crest cells leads to misalignment of the OFT with the ventricles, as observed in some *Hoxb1* mutant embryos. Cardiac defects caused by absence of *Hoxb1* are thus similar to those associated with cardiac neural crest ablation in chick embryos. Neural crest cells are derived from regions where Hoxb1 is early expressed as revealed by our previous Cre lineage analysis using $Hoxb1^{IRES\text{-}Cre}$; *R26R* mice (Bertrand et al., 2011). However, $Hoxb1^{-/-}$ embryos exhibit no defects in neural crest-derived tissues (Goddard et al., 1996; Studer et al., 1996), as confirmed here using AP-2α immunostaining. Although the number of neural

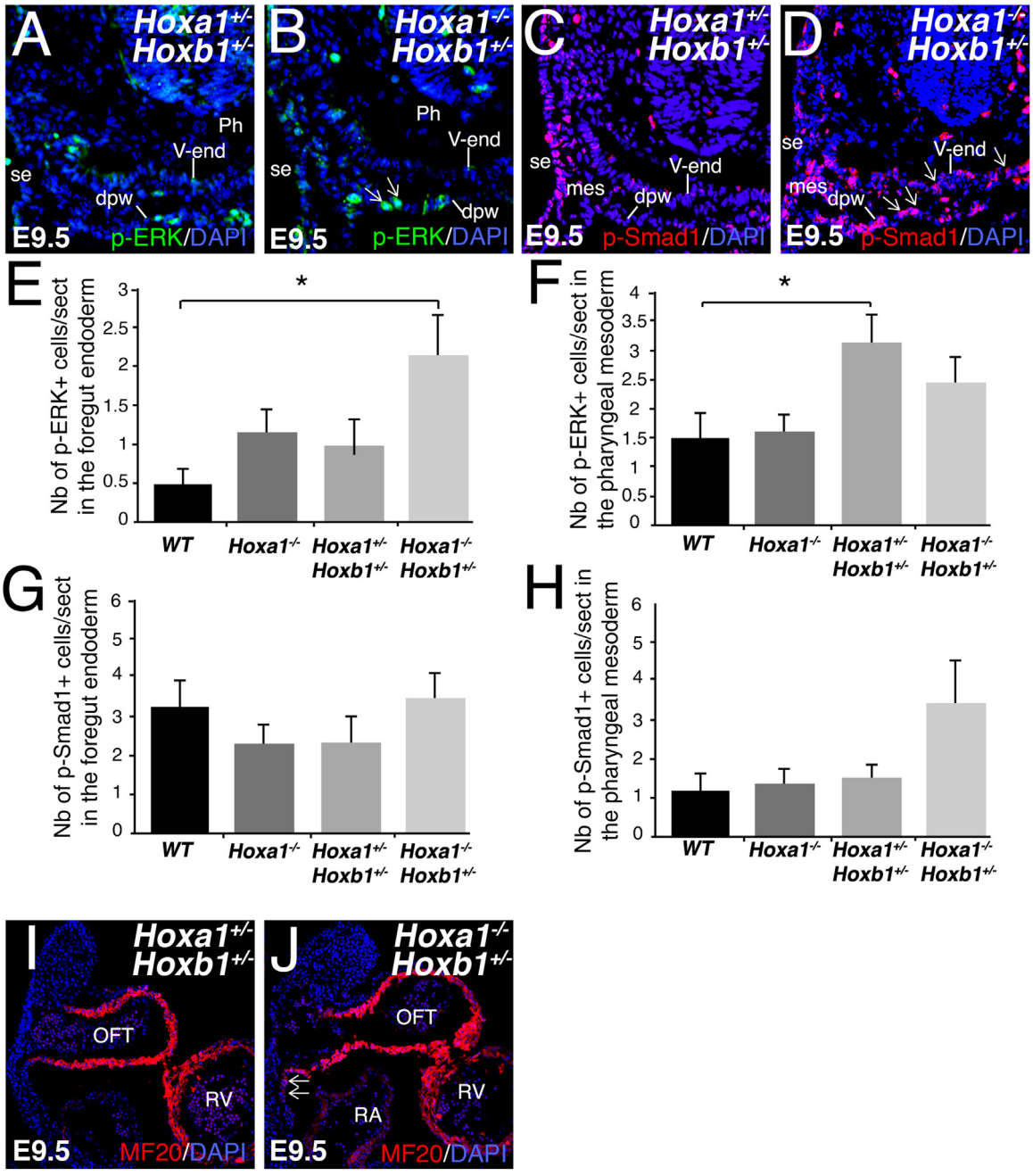

Fig. 6. FGF/ERK and BMP/SMAD signaling pathways are altered in$Hoxa1^{-/-};Hoxb1^{+/-}$ mutants. Immunochemistry on transverse (A)–(D) and sagittal (I) and (J) sections from $Hoxa1^{+/-}$; $Hoxb1^{+/-}$ (A,C,I) and $Hoxa1^{-/-}$; $Hoxb1^{+/-}$ (B), (D) and (J) embryos. (A) and (B) Immunochemistry with anti-phospho-ERK antibody (p-ERK, green) reveals increased number of p-ERK positive cells in the ventral pharyngeal endoderm and dorsal pericardial wall of $Hoxa1^{-/-};Hoxb1^{+/-}$ (arrows) compared to $Hoxa1^{+/-}$; $Hoxb1^{+/-}$ embryos. (C) and (D) Transverse section of $Hoxa1^{+/-};Hoxb1^{+/-}$ and $Hoxa1^{-/-};Hoxb1^{+/-}$ embryos at E9.5 immunostained for phospho-Smad1/5/8 (p-Smad1, red) showing robust p-Smad1 expression in the ventral endoderm and the dorsal pericardial wall of $Hoxa1^{-/-};Hoxb1^{+/-}$ embryos. (E)–(H) Histograms comparing the number of p-ERK- and p-Smad1-positive cells per section ($n=8$) in the pharyngeal endoderm (E) and (G) and mesoderm (F) and (H) of E9.5 *WT*, $Hoxa1^{-/-}$, $Hoxa1^{+/-};Hoxb1^{+/-}$ and $Hoxa1^{-/-};Hoxb1^{+/-}$ embryos. The quantification confirms an increased number of p-ERK-positive cells in the compound embryos compared to control or $Hoxa1^{-/-}$ embryos. Note the slight increase of p-Smad1-positive cells in the pharyngeal mesoderm of $Hoxa1^{-/-};Hoxb1^{+/-}$ vs. other genetic backgrounds ($^*p<0.05$, Student's *t* test). (I) and (J) Immunochemistry with anti-MF20 antibody (red) showing differentiated cells in the SHF of $Hoxa1^{-/-};Hoxb1^{+/-}$ embryos (arrows). Nuclei are labeled with DAPI (blue). dpw, dorsal pericardial wall; l-end; lateral endoderm; mes, pharyngeal mesenchyme; OFT, outflow tract; Ph, pharynx; RV, right ventricle; V-end, ventral pharyngeal endoderm; se, surface ectoderm.

crest-derived cells is not affected in *Hoxb1*$^{-/-}$, the interaction with surrounding pharyngeal cells is probably compromised due to alteration of major signaling pathways, including FGF and BMP signaling.

BMP/SMAD signaling regulates SHF differentiation (Hutson et al., 2010; Tirosh-Finkel et al., 2010; Wang et al., 2010). In addition, *Bmp4* is required for OFT septation (Liu et al., 2004). Although we did not detect significant changes in *Bmp4* transcript levels, we found an increase in the number of p-Smad1-positive cells in *Hoxb1*$^{-/-}$ embryos, suggesting that another BMP ligands might be involved in this up-regulation. However, the presence of p-Smad1 in the nucleus is not necessarily equivalent to BMP-induced transcriptional activity (Faure et al., 2002; Monteiro et al., 2004). Indeed, Smad6 can recruit transcriptional co-repressor CtBP to repress Smad1-induced transcription (Lin et al., 2003). Interestingly, another Hox protein, Hoxc8, has been shown to negatively regulate BMP-mediated gene expression through the activation of Smad6 (Kang et al., 2010). More studies are needed to further explore whether similar regulatory events occur during OFT development.

4.2. Abnormal presence of cardiomyocytes in the SHF of *Hoxb1*$^{-/-}$ and *Hoxa1*$^{-/-}$; *Hoxb1*$^{+/-}$ embryos

We observed the presence of ectopic cardiomyocytes in the pharyngeal mesoderm within the SHF caudal to the OFT in *Hoxb1*$^{-/-}$ and *Hoxa1*$^{-/-}$;*Hoxb1*$^{+/-}$ embryos. Premature differentiation of SHF cells may have different explanations. (1) The microenvironment of SHF cells is important for OFT morphogenesis. A recent study demonstrated that loss of N-cadherin results in premature differentiation of SHF progenitor cells (Soh et al., 2014), (2) Communication between pharyngeal mesoderm and neural crest cells regulates the differentiation and/or recruitment of SHF cells into OFT. At E9.5, neural crest cells are in close contact with both layers. Thus, deficient neural crest cells may send an abnormal signal to SHF mesodermal cells that promote premature differentiation of the cardiac progenitors as demonstrated by alterations of BMP signaling (Jia et al., 2007). Inversely, abnormal signals send by either the pharyngeal mesoderm or the endoderm can affect the neural crest cell behaviors and indirectly the differentiation of SHF cells, (3) Perturbation of the temporal sequence of the OFT movement and SHF differentiation can results in the abnormal presence of cardiomyocytes in the SHF. This problem may result from an alteration in SHF cell migration (Rana et al., 2014). Interestingly in *Hoxb1*$^{-/-}$, MF20-positive cells are located in a region of the SHF that normally contributes to OFT myocardium (Waldo et al., 2005b, 2001).

4.3. Loss of Hoxb1 affects the inferior wall of the OFT

The myocardial cells of the OFT contribute to the base of the great vessels (Bajolle et al., 2006; Waldo et al., 2005b). A previous study suggested that myocardial differences at the base of the aorta and pulmonary trunk are prefigured in distinct SHF cell populations (Bajolle et al., 2008). Our genetic tracing analysis using the *Hoxb1*$^{IRES\text{-}Cre}$ mouse line (Arenkiel et al., 2003) demonstrated a contribution of *Hoxb1*-expressing cells in the pSHF to the inferior wall of the OFT, which subsequently gives rise to subpulmonary myocardium (Bertrand et al., 2011). In addition, two studies using retrospective clonal analysis and DiI labeling experiments in the mouse support this notion (Dominguez et al., 2012; Lescroart et al., 2012). Our phenotypic analysis of *Hoxb1*$^{-/-}$ embryos using *y96-Myf5-nlacZ-16* (*96–16*) transgene reveals decreased X-gal positive cells at the inferior wall of the OFT which is consistent with the lineage studies. Previous work has revealed loss of this β-galactosidase domain and defective contribution of the *Hoxb1*$^{IRES\text{-}Cre}$ lineage to the OFT associated with common arterial trunk in *Tbx1* mutant hearts (Rana et al., 2014; Theveniau-Ruissy et al., 2008). However our results suggest a milder SHF defect in *Hoxb1*$^{-/-}$ embryos potentially due to functional redundancy with other *Hox* genes expressed in the pSHF including *Hoxa1* and *Hoxa3* (Bertrand et al., 2011).

4.4. Overlapping functions of Hoxa1 and Hoxb1 during OFT development

Heart defects resulting from loss of function of either *Hoxa1* or *Hoxb1* are different. *Hoxb1* mutant embryos have a shortened OFT that subsequently causes misalignment of the OFT and VSD. In contrast, although a low percentage of VSDs was observed, disruption of *Hoxa1* does not alter SHF deployment or the length of the OFT. These differences suggest distinct functions of these paralogous *Hox* genes during OFT development. However, reduction of the length of the OFT and increased incidence of heart defects are observed in compound *Hoxa1*$^{-/-}$;*Hoxb1*$^{+/-}$ embryos compared to *Hoxa1*$^{-/-}$ mutants, demonstrating an overlap in function between these two genes during OFT formation. Additionally, we detected an early disruption of FGF/ERK and BMP/SMAD signaling in the pharyngeal region of *Hoxa1*$^{-/-}$; *Hoxb1*$^{+/-}$ but not in *Hoxa1*$^{-/-}$ embryos. Hence, removing one copy of *Hoxb1* in the *Hoxa1*$^{-/-}$ background uncovers a requirement for Hoxa1 in cells that normally contribute to OFT development. Synergy between *Hoxa1* and *Hoxb1* has already been reported in early patterning of the hindbrain region (Gavalas et al., 1998; Rossel and Capecchi, 1999; Studer et al., 1998). One of these studies revealed that Hoxa1 plays a role in activating the *Hoxb1* r4-enhancer at early stages but does not participate in long-term maintenance of *Hoxb1* expression (Studer et al., 1998). However, the expression pattern of *Hoxb1* in the pharyngeal region appears normal in *Hoxa1* mutant embryos at E9.5 (data not shown). In summary, our study defines a novel role of *Hoxa1* in OFT progenitor cells, revealed only in the absence of Hoxb1.

Hoxa3 is expressed in posterior SHF cells that contribute to the inferior OFT wall (Bertrand et al., 2011; Diman et al., 2011). Hoxa3 is unlikely to compensate for the loss of both *Hoxa1* and *Hoxb1* since its expression is more posterior than that of both *Hoxa1* and *Hoxb1* and *Hoxa3* expression is unchanged in *Hoxa1*$^{-/-}$, *Hoxb1*$^{-/|-}$ embryos (Rossel and Capecchi, 1999). Interestingly, deletion of the *HoxA* and *HoxB* gene clusters in the mouse has uncovered the requirement of both *HoxA* and *HoxB* paralogs during heart looping (Soshnikova et al., 2013). Although less affected, heart morphology in double homozygous *Hoxa1; Hoxb1* embryos appears abnormal embryos appears abnormal (see Fig. 5). Together, these results confirm the importance of these two anterior *Hox* genes during heart development. Importantly, these defects may explain the early lethality observed in this genetic context (Supplementary material Table S1) (Gavalas et al., 1998; Rossel and Capecchi, 1999; Studer et al., 1998).

In summary, we have discovered a novel role of anterior *Hox* genes in OFT development. OFT defects in both *Hoxb1*$^{-/-}$ or *Hoxa1*$^{-/-}$; *Hoxb1*$^{+/-}$ embryos result in altered levels of FGF and BMP signaling. This in turn results in abnormal proliferation and premature differentiation of cardiac progenitors in the SHF caudal to the OFT. Thus, we hypothesize that mutations of human *HOXA1* and *HOXB1* may contribute to the pathogenesis of the conotruncal region in human patients.

Acknowledgments

We thank Anne Moon and Robert Kelly for their comments on the manuscript. This work was supported by the “Association

Française contre les Myopathies" [NMH-Decrypt Project], the "Agence Nationale pour la Recherche [ANR-13-BSV2-0003-01], and the "Institut National de la Santé et de la Recherche Médicale" to S.Z. M.R. received PhD fellowships from the "Ministère de l'Enseignement Supérieur et de la Recherche" and the "Association Française contre les Myopathies" [NMH-Decrypt]. B.L received postdoctoral fellowships from the "Fondation pour la Recherche Médicale" and the "Agence Nationale pour la Recherche [ANR-13-BSV2-0003].

Appendix A. Supplementary material

Supplementary data associated with this article can be found in the online version at http://dx.doi.org/10.1016/j.ydbio.2015.08.015.

References

Abu-Issa, R., Smyth, G., Smoak, I., Yamamura, K., Meyers, E.N., 2002. Fgf8 is required for pharyngeal arch and cardiovascular development in the mouse. Development 129, 4613–4625.
Arenkiel, B.R., Gaufo, G.O., Capecchi, M.R., 2003. Hoxb1 neural crest preferentially form glia of the PNS. Dev. Dyn. 227, 379–386.
Bajolle, F., Zaffran, S., Kelly, R.G., Hadchouel, J., Bonnet, D., Brown, N.A., Buckingham, M.E., 2006. Rotation of the myocardial wall of the outflow tract is implicated in the normal positioning of the great arteries. Circ. Res. 98, 421–428.
Bajolle, F., Zaffran, S., Meilhac, S.M., Dandonneau, M., Chang, T., Kelly, R.G., Buckingham, M.E., 2008. Myocardium at the base of the aorta and pulmonary trunk is prefigured in the outflow tract of the heart and in subdomains of the second heart field. Dev. Biol. 313, 25–34.
Bertrand, N., Roux, M., Ryckebusch, L., Niederreither, K., Dolle, P., Moon, A., Capecchi, M., Zaffran, S., 2011. Hox genes define distinct progenitor sub-domains within the second heart field. Dev. Biol. 353, 266–274.
Buckingham, M., Meilhac, S., Zaffran, S., 2005. Building the mammalian heart from two sources of myocardial cells. Nat. Rev. Genet 6, 826–835.
Cai, C.L., Liang, X., Shi, Y., Chu, P.H., Pfaff, S.L., Chen, J., Evans, S., 2003. Isl1 identifies a cardiac progenitor population that proliferates prior to differentiation and contributes a majority of cells to the heart. Dev. cell 5, 877–889.
Corson, L.B., Yamanaka, Y., Lai, K.M., Rossant, J., 2003. Spatial and temporal patterns of ERK signaling during mouse embryogenesis. Development 130, 4527–4537.
Diman, N.Y., Remacle, S., Bertrand, N., Picard, J.J., Zaffran, S., Rezsohazy, R., 2011. A retinoic acid responsive Hoxa3 transgene expressed in embryonic pharyngeal endoderm, cardiac neural crest and a subdomain of the second heart field. PloS one 6, e27624.
Dominguez, J.N., Meilhac, S.M., Bland, Y.S., Buckingham, M.E., Brown, N.A., 2012. Asymmetric fate of the posterior part of the second heart field results in unexpected left/right contributions to both poles of the heart. Circ. Res. 111, 1323–1335.
Duester, G., 2008. Retinoic acid synthesis and signaling during early organogenesis. Cell 134, 921–931.
Dyer, L.A., Kirby, M.L., 2009. The role of secondary heart field in cardiac development. Dev. Biol. 336, 137–144.
Farrell, M.J., Burch, J.L., Wallis, K., Rowley, L., Kumiski, D., Stadt, H., Godt, R.E., Creazzo, T. L., Kirby, M.L., 2001. FGF-8 in the ventral pharynx alters development of myocardial calcium transients after neural crest ablation. J. Clin. Invest. 107, 1509–1517.
Faure, S., de Santa Barbara, P., Roberts, D.J., Whitman, M., 2002. Endogenous patterns of BMP signaling during early chick development. Dev. Biol 244, 44–65.
Frank, D.U., Fotheringham, L.K., Brewer, J.A., Muglia, L.J., Tristani-Firouzi, M., Capecchi, M.R., Moon, A.M., 2002. An Fgf8 mouse mutant phenocopies human 22q11 deletion syndrome. Development 129, 4591–4603.
Galli, D., Dominguez, J.N., Zaffran, S., Munk, A., Brown, N.A., Buckingham, M.E., 2008. Atrial myocardium derives from the posterior region of the second heart field, which acquires left-right identity as Pitx2c is expressed. Development 135, 1157–1167.
Gaufo, G.O., Flodby, P., Capecchi, M.R., 2000. Hoxb1 controls effectors of sonic hedgehog and Mash1 signaling pathways. Development 127, 5343–5354.
Gavalas, A., Studer, M., Lumsden, A., Rijli, F.M., Krumlauf, R., Chambon, P., 1998. Hoxa1 and Hoxb1 synergize in patterning the hindbrain, cranial nerves and second pharyngeal arch. Development 125, 1123–1136.
Goddard, J.M., Rossel, M., Manley, N.R., Capecchi, M.R., 1996. Mice with targeted disruption of Hoxb-1 fail to form the motor nucleus of the VIIth nerve. Development 122, 3217–3228.
Hoffman, J.I., Kaplan, S., 2002. The incidence of congenital heart disease. J. Am. Coll. Cardiol. 39, 1890–1900.
Hutson, M.R., Zeng, X.L., Kim, A.J., Antoon, E., Harward, S., Kirby, M.L., 2010. Arterial pole progenitors interpret opposing FGF/BMP signals to proliferate or differentiate. Development 137, 3001–3011.
Hutson, M.R., Zhang, P., Stadt, H.A., Sato, A.K., Li, Y.X., Burch, J., Creazzo, T.L., Kirby, M.L., 2006. Cardiac arterial pole alignment is sensitive to FGF8 signaling in the pharynx. Dev. Biol. 295, 486–497.
Ilagan, R., Abu-Issa, R., Brown, D., Yang, Y.P., Jiao, K., Schwartz, R.J., Klingensmith, J., Meyers, E.N., 2006. Fgf8 is required for anterior heart field development. Development 133, 2435–2445.
Jia, Q., McDill, B.W., Li, S.Z., Deng, C., Chang, C.P., Chen, F., 2007. Smad signaling in the neural crest regulates cardiac outflow tract remodeling through cell autonomous and non-cell autonomous effects. Dev. Biol. 311, 172–184.
Kang, M., Bok, J., Deocaris, C.C., Park, H.W., Kim, M.H., 2010. Hoxc8 represses BMP-induced expression of Smad6. Mol. Cells. 29, 29–33.
Kelly, R.G., Brown, N.A., Buckingham, M.E., 2001. The arterial pole of the mouse heart forms from Fgf10-expressing cells in pharyngeal mesoderm. Dev. Cell 1, 435–440.
Kirby, M.L., Gale, T.F., Stewart, D.E., 1983. Neural crest cells contribute to normal aorticopulmonary septation. Science 220, 1059–1061.
Lescroart, F., Mohun, T., Meilhac, S.M., Bennett, M., Buckingham, M., 2012. Lineage tree for the venous pole of the heart: clonal analysis clarifies controversial genealogy based on genetic tracing. Circ. Res 111, 1313–1322.
Li, X., Lufkin, T., 2000. Cre recombinase expression in the floorplate, notochord and gut epithelium in transgenic embryos driven by the Hoxa-1 enhancer III. Genesis 26, 121–122.
Lin, X., Liang, Y.Y., Sun, B., Liang, M., Shi, Y., Brunicardi, F.C., Shi, Y., Feng, X.H., 2003. Smad6 recruits transcription corepressor CtBP to repress bone morphogenetic protein-induced transcription. Mol. Cell. Biol. 23, 9081–9093.
Liu, W., Selever, J., Wang, D., Lu, M.F., Moses, K.A., Schwartz, R.J., Martin, J.F., 2004. Bmp4 signaling is required for outflow-tract septation and branchial-arch artery remodeling. Proc. Natl. Acad Sci. U.S.A. 101, 4489–4494.
Lufkin, T., Dierich, A., LeMeur, M., Mark, M., Chambon, P., 1991. Disruption of the Hox-1.6 homeobox gene results in defects in a region corresponding to its rostral domain of expression. Cell 66, 1105–1119.
Makki, N., Capecchi, M.R., 2012. Cardiovascular defects in a mouse model of HOXA1 syndrome. Hum. Mol. Genet. 21, 26–31.
Mallo, M., Wellik, D.M., Deschamps, J., 2010. Hox genes and regional patterning of the vertebrate body plan. Dev. Biol. 344, 7–15.
Monteiro, R.M., de Sousa Lopes, S.M., Korchynskyi, O., ten Dijke, P., Mummery, C.L., 2004. Spatio-temporal activation of Smad1 and Smad5 in vivo: monitoring transcriptional activity of Smad proteins. J. Cell Sci. 117, 4653–4663.
Niederreither, K., Dolle, P., 2008. Retinoids and heart development. In: Rosenthal, N., Harvey, R.P. (Eds.), Academic Press, San Diego (Eds.).
Niederreither, K., Subbarayan, V., Dolle, P., Chambon, P., 1999. Embryonic retinoic acid synthesis is essential for early mouse post-implantation development. Nat. Genet 21, 444–448.
Niederreither, K., Vermot, J., Messaddeq, N., Schuhbaur, B., Chambon, P., Dolle, P., 2001. Embryonic retinoic acid synthesis is essential for heart morphogenesis in the mouse. Development 128, 1019–1031.
Park, E.J., Ogden, L.A., Talbot, A., Evans, S., Cai, C.L., Black, B.L., Frank, D.U., Moon, A. M., 2006. Required, tissue-specific roles for Fgf8 in outflow tract formation and remodeling. Development 133, 2419–2433.
Porras, D., Brown, C.B., 2008. Temporal-spatial ablation of neural crest in the mouse results in cardiovascular defects. Dev. Dyn. 237, 153–162.
Prall, O.W., Menon, M.K., Solloway, M.J., Watanabe, Y., Zaffran, S., Bajolle, F., Biben, C., McBride, J.J., Robertson, B.R., Chaulet, H., Stennard, F.A., Wise, N., Schaft, D., Wolstein, O., Furtado, M.B., Shiratori, H., Chien, K.R., Hamada, H., Black, B.L., Saga, Y., Robertson, E.J., Buckingham, M.E., Harvey, R.P., 2007. An Nkx2-5/Bmp2/Smad1 negative feedback loop controls heart progenitor specification and proliferation. Cell 128, 947–959.
Rana, M.S., Theveniau-Ruissy, M., De Bono, C., Mesbah, K., Francou, A., Rammah, M., Dominguez, J.N., Roux, M., Laforest, B., Anderson, R.H., Mohun, T., Zaffran, S., Christoffels, V.M., Kelly, R.G., 2014. Tbx1 coordinates addition of posterior second heart field progenitor cells to the arterial and venous poles of the heart. Circ. Res. 115, 790–799.
Rochais, F., Mesbah, K., Kelly, R.G., 2009. Signaling pathways controlling second heart field development. Circ. Res 104, 933–942.
Rossel, M., Capecchi, M.R., 1999. Mice mutant for both Hoxa1 and Hoxb1 show extensive remodeling of the hindbrain and defects in craniofacial development. Development 126, 5027–5040.
Ryckebusch, L., Bertrand, N., Mesbah, K., Bajolle, F., Niederreither, K., Kelly, R.G., Zaffran, S., 2010. Decreased levels of embryonic retinoic acid synthesis accelerate recovery from arterial growth delay in a mouse model of DiGeorge syndrome. Circ Res 106, 686–694.
Ryckebusch, L., Wang, Z., Bertrand, N., Lin, S.C., Chi, X., Schwartz, R., Zaffran, S., Niederreither, K., 2008. Retinoic acid deficiency alters second heart field formation. Proc. Natl. Acad. Sci. U. S. A. 105, 2913–2918.
Soh, B.S., Buac, K., Xu, H., Li, E., Ng, S.Y., Wu, H., Chmielowiec, J., Jiang, X., Bu, L., Li, R. A., Cowan, C., Chien, K.R., 2014. N-cadherin prevents the premature differentiation of anterior heart field progenitors in the pharyngeal mesodermal microenvironment. Cell Res. 24, 1420–1432.
Soriano, P., 1999. Generalized lacZ expression with the ROSA26 Cre reporter strain. Nat. Genet. 21, 70–71.
Soshnikova, N., Dewaele, R., Janvier, P., Krumlauf, R., Duboule, D., 2013. Duplications of hox gene clusters and the emergence of vertebrates. Dev. Biol. 378, 194–199.
Studer, M., Gavalas, A., Marshall, H., Ariza-McNaughton, L., Rijli, F.M., Chambon, P., Krumlauf, R., 1998. Genetic interactions between Hoxa1 and Hoxb1 reveal new roles in regulation of early hindbrain patterning. Development 125, 1025–1036.
Studer, M., Lumsden, A., Ariza-McNaughton, L., Bradley, A., Krumlauf, R., 1996. Altered segmental identity and abnormal migration of motor neurons in mice lacking Hoxb-1. Nature 384, 630–634.
Sun, Y., Liang, X., Najafi, N., Cass, M., Lin, L., Cai, C.L., Chen, J., Evans, S.M., 2007. Islet

1 is expressed in distinct cardiovascular lineages, including pacemaker and coronary vascular cells. Dev. Biol. 304, 286–296.
Theveniau-Ruissy, M., Dandonneau, M., Mesbah, K., Ghez, O., Mattei, M.G., Miquerol, L., Kelly, R.G., 2008. The del22q11.2 candidate gene Tbx1 controls regional outflow tract identity and coronary artery patterning. Circ. Res. 103, 142–148.
Tirosh-Finkel, L., Zeisel, A., Brodt-Ivenshitz, M., Shamai, A., Yao, Z., Seger, R., Domany, E., Tzahor, E., 2010. BMP-mediated inhibition of FGF signaling promotes cardiomyocyte differentiation of anterior heart field progenitors. Development 137, 2989–3000.
Verzi, M.P., McCulley, D.J., De Val, S., Dodou, E., Black, B.L., 2005. The right ventricle, outflow tract, and ventricular septum comprise a restricted expression domain within the secondary/anterior heart field. Dev. Biol 287, 134–145.
Vincent, S.D., Buckingham, M.E., 2010. How to make a heart: the origin and regulation of cardiac progenitor cells. Curr. Top. Dev. Biol. 90, 1–41.
Vitelli, F., Taddei, I., Morishima, M., Meyers, E.N., Lindsay, E.A., Baldini, A., 2002. A genetic link between Tbx1 and fibroblast growth factor signaling. Development 129, 4605–4611.
Waldo, K.L., Hutson, M.R., Stadt, H.A., Zdanowicz, M., Zdanowicz, J., Kirby, M.L., 2005a. Cardiac neural crest is necessary for normal addition of the myocardium to the arterial pole from the secondary heart field. Dev. Biol 281, 66–77.
Waldo, K.L., Hutson, M.R., Ward, C.C., Zdanowicz, M., Stadt, H.A., Kumiski, D., Abu-Issa, R., Kirby, M.L., 2005b. Secondary heart field contributes myocardium and smooth muscle to the arterial pole of the developing heart. Dev. Biol. 281, 78–90.
Waldo, K.L., Kumiski, D.H., Wallis, K.T., Stadt, H.A., Hutson, M.R., Platt, D.H., Kirby, M. L., 2001. Conotruncal myocardium arises from a secondary heart field. Development 128, 3179–3188.
Wang, J., Greene, S.B., Bonilla-Claudio, M., Tao, Y., Zhang, J., Bai, Y., Huang, Z., Black, B.L., Wang, F., Martin, J.F., 2010. Bmp signaling regulates myocardial differentiation from cardiac progenitors through a MicroRNA-mediated mechanism. Dev. Cell 19, 903–912.
Ward, C., Stadt, H., Hutson, M., Kirby, M.L., 2005. Ablation of the secondary heart field leads to tetralogy of Fallot and pulmonary atresia. Dev. Biol. 284, 72–83.
Watanabe, Y., Miyagawa-Tomita, S., Vincent, S.D., Kelly, R.G., Moon, A.M., Buckingham, M.E., 2010. Role of mesodermal FGF8 and FGF10 overlaps in the development of the arterial pole of the heart and pharyngeal arch arteries. Circ. Res. 106, 495–503.
Wellik, D.M., 2009. Hox genes and vertebrate axial pattern. Curr. Top. Dev. Biol. 88, 257–278.
Zaffran, S., Kelly, R.G., 2012. New developments in the second heart field. Differ.: Res. Biol. Div. 84, 17–24.
Zaffran, S., Kelly, R.G., Meilhac, S.M., Buckingham, M.E., Brown, N.A., 2004. Right ventricular myocardium derives from the anterior heart field. Circ. Res. 95, 261–268.
Zammit, P.S., Kelly, R.G., Franco, D., Brown, N., Moorman, A.F., Buckingham, M.E., 2000. Suppression of atrial myosin gene expression occurs independently in the left and right ventricles of the developing mouse heart. Dev. Dyn. 217, 75–85.